Annals of Botany **132**: 869–879, 2023
https://doi.org/10.1093/aob/mcad070, available online at www.academic.oup.com/aob

ANNALS OF BOTANY
Founded 1887

PART OF A SPECIAL ISSUE ON CAM AT THE CROSSROADS

Developmental dynamics of crassulacean acid metabolism (CAM) in *Opuntia ficus-indica*

Nicholas A. Niechayev[1], Jesse A. Mayer[2] and John C. Cushman[3,*]

[1]Department of Seed Research, D'Arrigo California, 21777 Harris Road, Salinas, CA 93908, USA, [2]Biosero Inc., 9560 Waples Street, San Diego, CA 92121, USA and [3]Department of Biochemistry and Molecular Biology, University of Nevada, Reno, NV 89557-0330, USA
**For correspondence. E-mail jcushman@unr.edu*

Received: 25 January 2023 Returned for revision: 10 May 2023 Editorial decision: 24 May 2023 Accepted: 26 May 2023

• **Background and Aims** The relative contributions of C_3 photosynthesis and crassulacean acid metabolism (CAM) during the earliest stages of development were investigated to assess how much each might contribute to cactus pear (*Opuntia ficus-indica*) productivity.
• **Methods** The developmental progression of C_3 photosynthesis and CAM was assessed in seedlings and daughter cladodes of mature plants by titratable acidity, $\delta^{13}C$ isotopic values and diel gas exchange measurements.
• **Key Results** Nocturnal acidification was observed in seedling cladodes and cotyledons at the earliest stages of development and became highly significant by 75 days of development. Seedling cotyledons showed mean $\delta^{13}C$ values of −21.4 and −17.1 ‰ at 30 and 100 days of age, respectively. Seedling cladodes showed mean $\delta^{13}C$ values of −19.4 and −14.5 ‰ at 30 and 100 days of age, respectively. These values are typical of CAM plants. Net CO_2 assimilation was negative, then occurred in both the day and the night, with nighttime fixation becoming predominant once the primary cladode reached 5 cm in size. Emergent daughter cladodes growing on mature plants showed nocturnal titratable acidity at the earliest stages of development, which became significant when daughter cladodes were >2.5–5 cm in height. Emergent daughter cladodes showed mean $\delta^{13}C$ values of −14.5 to −15.6 ‰, typical of CAM plants. CO_2 assimilation studies revealed that net CO_2 uptake was negative in daughter cladodes <12 cm in length, but then exhibited net positive CO_2 assimilation in both the day and the night, with net nocturnal CO_2 assimilation predominating once the daughter cladode grew larger.
• **Conclusions** Developing *O. ficus-indica* primary and daughter cladodes begin as respiring sink tissues that transition directly to performing CAM once net positive CO_2 fixation is observed. Overall, these results demonstrate that CAM is the primary form of photosynthetic carbon assimilation for *O. ficus-indica* even at the earliest stages of seedling or daughter cladode development.

Key words: Cactus pear, *Opuntia ficus-indica*, crassulacean acid metabolism, seedlings, daughter cladodes, phosphoenolpyruvate carboxylase, developmental physiology, germination, gas exchange, photosynthesis, $\delta^{13}C$ values.

INTRODUCTION

Crassulacean acid metabolism (CAM) is a mode of photosynthesis in which stomata open at night for carbon uptake and transpiration instead of during the day, as is the case in C_3 and C_4 photosynthetic plants. Diel CO_2 uptake in CAM plants consists of four separate phases spanning a 24 h diel cycle (Osmond, 1978; Winter, 1985). Phase I occurs at night, when stomata are open, allowing CO_2 uptake and primary fixation after its conversion to HCO_3^- by carbonic anhydrase (CA) and phosphoenolpyruvate (PEP) carboxylase (PEPC). PEPC uses PEP as the three-carbon acceptor derived from storage carbohydrates via glycolysis to generate four-carbon oxaloacetate (OAA), which is rapidly reduced to malate, then transported and stored in the vacuole overnight as malic acid. The nocturnal accumulation of malic acid is one of the defining features of CAM plants (Winter and Smith, 2022). The other three phases occur during the day. In the early morning, during the transitional phase II, with stomata still open, the combined activities of PEPC and light-activated ribulose-1,5-bisphosphate carboxylase/oxygenase (RuBisCO) can result in a burst of CO_2 fixation. During phase III, the stored malic acid is released from the vacuole and decarboxylated in the cytosol by NAD(P)-malic enzyme coupled with pyruvate, orthophosphate dikinase or PEP carboxykinase, depending upon the CAM species (Christopher and Holtum, 1996). Stomata close, resulting in little to no net CO_2 assimilation, and the released CO_2 is refixed by the Calvin–Benson–Bassham cycle as in the normal C_3 photosynthetic pathway. During this phase, the released pyruvate or PEP, depending upon the decarboxylation pathway, is recycled to stored carbohydrates via gluconeogenesis (Christopher and Holtum, 1996, 1998). Near the end of the day, as malate stores are exhausted, phase IV is marked by stomatal reopening, presumably owing to a decline in intracellular CO_2 concentrations and a second burst of net CO_2 fixation, which can occur by the combined actions of

PEPC and RuBisCO, depending upon the prevailing environmental conditions.

CAM plants are extremely plastic in their engagement of the CAM pathway, depending upon their evolutionary history, developmental status and environmental conditions (Winter *et al.*, 2015). CAM occurs in several different modes, spanning a range from 0 to 100 % net nocturnal CO_2 fixation per 24 h period. CAM cycling describes plants in which diel organic acid fluctuations from the recapture of respiratory CO_2 are detectable but lack net nocturnal CO_2 fixation (Martin, 1996; Herrera, 2008). Plants expressing low-level CAM or weak CAM or C_3–CAM display detectable diel organic acid fluctuations and $\delta^{13}C$ values that range from −26 to −20 ‰, where a value of −20 ‰ corresponds to a contribution of ~40 % total carbon gain derived from net nocturnal CO_2 fixation (Winter and Holtum, 2002). In contrast, strong, obligate or constitutive CAM plants, which rely heavily upon nocturnal CO_2 uptake and fixation, typically display $\delta^{13}C$ values from −20 to −8 ‰. Extensive $\delta^{13}C$ value surveys from many plant families have revealed clear bimodal distributions of $\delta^{13}C$ values, reflecting either the performance of C_3 photosynthesis or strong CAM (Messerschmid *et al.*, 2021). However, the subfamily Mesembryanthemoideae (Aizoaceae) displayed a continuous, unimodal distribution of $\delta^{13}C$ values across a wide range (between −30 and −8 ‰), with a mean of −19 (±4.3) ‰, which suggests that the use of $\delta^{13}C$ values as thresholds for defining CAM is potentially misleading (Messerschmid *et al.*, 2021). The transitional zone between the bimodal distributions of C_3 photosynthesis and CAM spanning −23 to −19 ‰ has been defined as the Winter–Holtum zone (Males, 2018; Niechayev *et al.*, 2019).

The transition from C_3 photosynthesis to CAM can be under developmental control in constitutive CAM species (Jones, 1975; Nishida, 1978). For example, the young developing leaves of *Kalanchoe pinnata* perform predominantly C_3 photosynthesis, whereas more mature leaves transition developmentally to CAM, as assessed by changing RuBisCO/PEPC activity ratios (Winter *et al.*, 1982). This developmental transition has made *Kalanchoe* species excellent models to dissect the genetic requirements for CAM (Winter *et al.*, 2008; Dever *et al.*, 2015; Hartwell *et al.*, 2016; Boxall *et al.*, 2017, 2020; Yang *et al.*, 2017). The developmental gradient of CAM has also been described in *Clusia* spp. (Walter *et al.*, 2008; Winter *et al.*, 2008), pig's ear (*Cotyledon orbiculate*) (Barker *et al.*, 1997), pineapple (*Ananas comosus*) (Ming *et al.*, 2015; Wai *et al.*, 2017) and moth orchid (*Phalaenopsis aphrodite*) (Ping *et al.*, 2018) to improve our understanding of the functional and evolutionary requirements for CAM.

The developmental regulation of CAM has also been studied in several cactus pear species, namely *Opuntia ficus-indica* (Winter *et al.*, 2008) and *O. elatior* (Winter and Holtum, 2011). *Opuntia ficus-indica* is described as a strong, obligate or constitutive CAM species, with $\delta^{13}C$ values of −13.6 to −11.7 ‰ in mature cladodes under ambient CO_2 levels (Ziegler, 1996; Nogués *et al.*, 2008). Other members of the *Opuntia* genus display *in situ* $\delta^{13}C$ values that range from −14.9 to −10.4 ‰ (Osmond *et al.*, 1979; Mooney *et al.*, 1989; Skrzypek *et al.*, 2013). *Opuntia ficus-indica* and related species (e.g. *Opuntia basilaris* and *Opuntia stricta*) typically grow in arid environments and in *in situ* conditions display little or no net CO_2 uptake during the day, corresponding to CAM phases II (early morning), III (daytime) and IV (late evening), with most net CO_2 uptake occurring at night (CAM phase I) (Nogués *et al.*, 2008; Osmond *et al.*, 2008). Daughter cladodes (flattened stem segments) start out as sinks after 14–18 days, requiring carbohydrate import for growth, but then transition to become source tissues after 27–28 days of development (Wang *et al.*, 1998). Initially, the daughter cladodes show more CO_2 respiration than assimilation and begin to show net CO_2 assimilation at ~20 days after their appearance. However, very young apical cladodes (~3 cm) of *O. ficus-indica* display positive net CO_2 fixation in both the dark and the light, with water-deficit stress resulting in a strong increase in dark CO_2 fixation and a decrease in light CO_2 fixation (Winter *et al.*, 2008). Rewatering of the mother cladode resulted in a return of both net dark and light CO_2 uptake. These results demonstrated that even species that are regarded as constitutive CAM can exhibit aspects of facultative CAM.

In a related study with a tropical, epiphytic cactus species, *Opuntia elatior* Mill., the cotyledons of young seedlings were shown to fix CO_2 in the light, following a C_3 photosynthesis gas exchange pattern (Winter and Holtum, 2011). As the primary cladode developed, a C_3 photosynthesis gas exchange pattern was observed until the cladode reached 10 cm in height, with detectable net nighttime CO_2 exchange and nocturnal acid accumulation evident in the emerging cladode. However, when water-deficit stress was applied to the seedlings, net dark CO_2 and nocturnal acid accumulation was induced, indicative of facultative CAM. Rewatering of the seedlings resulted in a rapid recovery of daytime carbon gain, whereas nighttime CO_2 uptake decreased transiently. These results showed that net CO_2 fixation occurred throughout the 24 h diel cycle and that a facultative component of CAM was present in this constitutive CAM species.

We wanted to understand the extent to which the C_3 photosynthetic pathway during early development might explain the high productivity of this obligate CAM species (Borland *et al.*, 2009; Neupane *et al.*, 2021). Therefore, we quantified the occurrence of C_3 photosynthesis and CAM in developing *O. ficus-indica* seedlings using dawn and dusk tissue acidity, $\delta^{13}C$ values and 24 h gas exchange to determine the relative contribution of each pathway to net CO_2 uptake. The developmental progression of CAM was also monitored in daughter cladodes of *O. ficus-indica* using the same analytical approaches. Our results showed that *O. ficus-indica* primary seedling and daughter cladodes behave as respiring sink tissues during the very early stages of development, transitioning to CAM for photosynthetic carbon assimilation thereafter.

MATERIALS AND METHODS

Seed collection and cleaning

To produce seeds for experimentation, 4-year-old *O. ficus-indica* plants were transferred from 11.3 L pots to 50 L pots in a 4:1 ratio of Sunshine MVP soil mix (Sun Gro Horticulture, Agawam, MA, USA) and natural play sand (SAKRETE, Charlotte, NC, USA) in the University of Nevada, Reno Valley Road Greenhouse Complex. Plants were given 200 g of Osmocote® (N–P–K 14–14–14, The Scotts Company,

Marysville, OH, USA) as fertilizer and 8 g of systemic insecticide treatment (Marathon® 1 % G Granular, OHP, Morrisville, NC, USA) every 6 months to control for insects. Standard greenhouse conditions with natural light were ~1100–1500 μmol m^{-2} s^{-1}, and the temperature ranged from 28–32 °C during the day to 17–18 °C at night. In May, flowers were pollinated using cotton swabs. Over the following months, fully mature fruits were collected for seed extraction.

Seed extraction was performed by removing the peel with a razor blade. The excess pulp was separated by hand, and the remaining seed–pulp mixture was placed in a stainless-steel mesh colander (8.25 cm, 2133, Norpro, Everett, WA, USA) and rinsed. Seeds were then placed into a 500 mL beaker (one per fruit) filled with distilled water at room temperature with a stir bar and stirred for 24 h. Seeds were rinsed with fresh distilled water daily over a period of several days until all carpel material was removed from the seeds. Seeds were blotted dry with a paper towel, allowed to dry completely, and stored in 50 mL conical centrifuge tubes (#352070, Corning™ Falcon® brand, Fisher Scientific, Suwanee, GA, USA). Cleaned seeds were allowed to age for ≥2 years before use.

Seed sterilization and germination

Seeds were surface sterilized in a solution of 10 % v/v household bleach and 0.5 % v/v Triton X-100 for 10 min with stirring in a volume of 10 mL of solution per seed. The seeds were transferred to a laminar flow hood, rinsed three times with sterile, deionized water, then rinsed with 100 % absolute ethanol (Koptec V1016, Decon Labs, King of Prussia, PA, USA) and allowed to air dry. After drying, seeds were clipped with ethanol/flame-sterilized fingernail clippers (Revlon®, New York, NY, USA) to remove ~75 % of the outer edge of the seed coat, without cutting into the embryo, to allow the seedling to emerge from the seed coat. Clipped seeds were then submerged in germination media containing either 3.0 % w/v sucrose, 0.6 % w/v Phyto agar (PTP01, Caisson Labs, Smithfield, UT, USA), 0.5 % w/v Murashige & Skoog medium with Gamborg's B5 vitamins (M404, PhytoTechnology Laboratories, Lenexa, KS, USA) and 10 mM gibberellic acid (G-120-50, Gold Biotechnology, St. Louis, MO, USA) or the same media containing no sucrose in 25 mm × 100 mm sterile polycarbonate Petri dishes (#89107-632, VWR™ brand, Avantor®, Radnor, PA, USA). Seeds were germinated in a tissue culture growth chamber (AR-7522, Percival Scientific, Derry, IA, USA) under a 16 h day–8 h night photoperiod, with ~80 μmol m^{-2} s^{-1} provided by fluorescent lamps at a constant temperature of 24 °C. The percentage and timing of seed germination were recorded. After 2 weeks, the seedlings were transferred to fresh plates containing the same media, but without gibberellic acid.

Titratable acidity analysis

Opuntia ficus-indica seedlings were sampled destructively at 30, 50, 75 and 100 days post-germination for tissue titratable acidity measurements. Seedlings were harvested, separated into cladode and cotyledon tissues, then weighed. For titratable acidity, seedlings were harvested at dusk and dawn and immediately flash frozen in liquid N_2. The dawn/dusk titratable acidity was then analysed as described (Gehrig *et al.*, 2005), with slight modifications. Briefly, samples were placed in 25 mL beakers with 20 mL of 50 % v/v methanol and heated until the water reached a minimum of 80 °C and all methanol boiled off. Boiled samples were cooled to room temperature and brought back to 10 mL with deionized water. For each sample, the initial pH was recorded and then titrated to pH 7 for malate equivalent or to pH 8.4 for citrate equivalents or 10 if the previous pH points were missed. All samples were titrated with 5 mM KOH.

The H^+ equivalent was calculated as follows:

$$H = v\left(\frac{0.01}{w}\right) \times 1000$$

where H is the H^+ equivalent, v the volume at the pH under consideration, and w the fresh weight of the sample.

Isotopic mass spectrometric analysis

Opuntia ficus-indica seedlings were sampled destructively after 30, 50, 75 and 100 days post-germination, separated into cladode and cotyledon tissues, then weighed. For $\delta^{13}C$ isotope measurements, samples were harvested at noon, lyophilized for 72 h in a LabConCo Freeze Dry System (Freezone 18, Kansas City, MO, USA), and pulverized using a BeadBlaster Microtube Homogenizer (D2400, Benchmark Scientific, Sayreville, NJ, USA). Between 2 and 3 mg of tissue was then loaded into tins (Item #041070, Costech Analytical Technologies, Valencia, CA, USA), placed into a 96-well plate, and shipped to either the Facility for Isotope Ratio Mass Spectrometry (FIRMS) located at the University of California, Riverside (https://ccb.ucr.edu/facilities/firms) or the Stable Isotope Facility (SIF) located at the University of California, Davis (http://icpms.ucdavis.edu/facilities-procedures) for the analysis of the ratio of ^{12}C and ^{13}C isotopes ($\delta^{13}C$) in each sample using Vienna Pee Dee Belemnite (VPDB) as the reference standard.

Seedling gas exchange measurements

After germination, seedlings with fully emerged cotyledons were transferred from tissue culture media to 65 mm LI-COR pots (Item #610-09646, LI-COR Environmental, Lincoln, NE, USA) with autoclaved Sunshine MVP soil mix (Sun Gro Horticulture, Agawam, MA, USA). The seedlings in pots were placed in a plastic container with sterilized water to a depth of 3 cm to allow the soil to take up water through the drainage holes and maintain soil holding capacity without changing the soil level. Plants were maintained on a custom-built fluorescent light rack and moved closer or further away from the light source to maintain a photosynthetically active radiation (PAR) of either 100 or 300 μmol m^{-2} s^{-1}, depending upon the experiment. Seedlings were measured for cotyledon size, central cladode size and stem height and photographed.

In the first set of experiments, gas exchange was recorded over a 48 h period in two separate 24 h (1440 min) measurements using the LI-COR 6400XT portable photosynthesis system, with the whole plant *Arabidopsis* chamber with clear top attached. In the first measurement, the LI-COR mixer was set to hold the sample chamber CO_2 at 400 μmol mol^{-1}, the flow rate was set to 500 μmol s^{-1}, the leaf fan to fast (setting 5),

block temperature was set to 20 °C, and the PAR at plant level was 100 µmol m^{-2} s^{-1}, with a 12 h day–12 h night photoperiod. The auto program (auto log 2) was set to log photo once every 5 min for 1440 min and match after every log. Desiccant (Item #2088701, LI-COR) and soda lime (Item #9964-090, LI-COR) were changed every 4 h. Humidity was held between 50 and 70 % within the sample period. Interference from root respiration was avoided by using a LI-COR 6400 exhaust set-up that forces air flow down through the soil by restricting 50 % of the exhaust flow (see figure 2 in: https://www.licor.com/documents/89lw0pf0ooypx3wgfmnr). The air forced down into the soil was pushed out of six small holes made with a hot needle, ~6 cm down from the lip of the pots. Before beginning the second measurement, the exhaust valve was turned to restrict air flow by 100 %, and the air flow was set to the maximum with desiccant on full scrub for 1 h until the soil in the pot was fully dried. Recording the wet and dry weight of the 65 mm pots with soil and seedlings revealed that pots held ~30 g of water at saturation.

The second set of experiments was conducted using a different set of seedlings. All settings were kept the same, with the exception that well-watered seedlings were acclimated and measured at a PAR of 300 µmol m^{-2} s^{-1} at the plant level, and each measurement was conducted for only 24 h. The LI-COR 6800XT with 6800-17 small plant chamber (see figures 1 and 2 in: https://www.licor.com/documents/eg2bp3sqbr4a97wjwhvupgigqter9zic) was used instead, following factory guidelines, with a flow rate of 800 µmol s^{-1}, pressure valve set to 0.2 kPa, relative air humidity to 50 %, sample CO_2 to 400 µmol mol^{-1}, fan speed of 10 000 rpm, and a block temperature of 20 °C. The auto-logged data were collected once every 5 min for 1440 min, with matching after each log point. The LI-COR 6800XT also used a system for pushing air down through the soil, but instead of holes in the side of the pot, an adjustable silicon exhaust cup was attached to the bottom of the pot, allowing a measured 20 % leak value.

Daughter cladode titratable acidity measurements

To determine daily nocturnal acidity build-up in daughter cladodes, 4-year-old *O. ficus-indica* individuals in 11.3 L pots at the University of Nevada, Reno Valley Road Greenhouse Complex were selected for analysis under greenhouse conditions with natural daytime light at ~1100–1500 µmol m^{-2} s^{-1} and the temperature at 28–32 °C during the day and 17–18 °C at night, with gradual sunup and sundown. A 10 mm cork borer (Fisher Scientific) was used to take samples of cladodes within different length categories ranging from 2 to 35 cm in length. In May 2016, tissues were collected at the appropriate dusk and dawn times and immediately weighed and flash frozen. Titratable acidity was measured and calculated as described above.

Daughter cladode isotopic mass spectrometric analysis

A parallel set of samples was collected in May 2017 at noon from the same length categories using a 10 mm cork borer (Fisher Scientific) as described above. These samples were weighed and immediately lyophilized as described above. The freeze-dried samples were then pulverized with a bead beater, and 2–3 mg of each sample was prepared for shipment to the FIRMS or SIF facility as described above for *O. ficus-indica* seedlings.

Daughter cladode gas exchange measurements

To measure the rate and duration of photosynthesis in growing daughter cladodes, emerging 2.5-cm-long cladodes were placed in a clear Plexiglass chamber (a cylinder 30 cm tall and 17 cm wide) custom fabricated by Tripp Plastics, Reno, NV, USA and connected to the LI-COR 6400XT (Supplementary data Fig. S1). The node of the daughter cladode was placed flush with the base of the chamber, and putty (21-601, Ideal Industries, Sycamore, IL, USA) was used to seal any air gaps around the emergent cladode. The LI-COR mixer was set to hold the reference chamber CO_2 at 400 µmol mol^{-1}, the flow rate was set to 700 µmol s^{-1}, the leaf fan to fast (setting 5), block temperature was set to 25 ° C, and the ambient PAR was measured with the LI-COR 6400XT external light sensor placed in a level position above the chamber with putty. At the beginning of each measurement, the length of the cladode was measured by looking across a measured grid on each side of the custom chamber. The LI-COR 6400XT was set to auto log every 10 min for 1440 min while matching once every 30 min. Measurements were repeated daily until the cladode grew too large to fit in the chamber (~15 cm in length). Changes in [CO_2] measured in parts per million (ΔCO_2, ppm) were calculated by subtracting the sample chamber [CO_2] from the reference chamber [CO_2]. All cladodes were measured when new cladodes were flushing between 3 April and 22 June 2017.

Statistical analyses

All statistical analysis and data visualization was performed using PRISM 9 software (GraphPad Software, Inc., San Diego, CA, USA), except for plots and calculations for cladode length growth rate, which were performed using Excel software (Microsoft, Redmond, WA, USA). A three-way ANOVA was performed to determine whether any significant variance was attributable to differences in tissue type, time of day, and seedling or cladode age, or any interactions among these variables. Welch's *t*-test was conducted to determine whether significant differences were evident in nocturnal tissue acidity within each tissue type collected at dusk and dawn for each age group (eight independent comparisons) (n = 5–10 for each category).

Seedling $\delta^{13}C$ isotope data were derived for each tissue type and age group (30, 50, 75 and 100 days after germination; n = 6 for each category). Simple linear regression analysis was used to determine whether the slopes of the two tissue types over their age were different. Before analysis, the various data groups were analysed and found to display normal distribution and heteroscedastic variance, hence the appropriate statistical tests were applied. A two-way ANOVA was conducted to determine whether any significant variance in $\delta^{13}C$ per mille (‰) vs. VPDB occurred owing to differences in tissue type and age or to an interaction between tissue type and age. Welch's *t*-test was used to determine whether significant differences in $\delta^{13}C$ ‰ vs.

VPDB occurred between tissue types within each age group (four independent comparisons).

Daughter cladode titratable acidity was grouped into eight different size categories (0–2.5, 2.5–5, 5–10, 10–15, 15–20, 20–25, 25–30 and 30–35 cm) in cladode height, with separate dawn and dusk tissue acidity measured in each category. Welch's *t*-tests were performed to determine whether a statistical difference occurred between dawn and dusk acidity in each category (eight independent comparisons) (n = 2–6 for each category).

Daughter cladode $\delta^{13}C$ values were derived from cladodes from eight different size categories (0–2, 2–4, 4–6, 6–8, 8–10, 10–12, 12–14 and 14–16 cm) and adult cladodes (n = 6 for each category). Cladodes in the adult category were fully matured cladodes that were ≥35 cm in length. Simple linear regression analysis was used to determine how daughter cladode $\delta^{13}C$ values varied over time. A one-way ANOVA was also conducted to determine whether any variance in measured $\delta^{13}C$ ‰ vs. VPDB occurred across the size categories. A follow-up Tukey's multiple comparisons test was used to reveal any groupings among size categories in relationship to measured $\delta^{13}C$ ‰ vs. VPDB.

Gas exchange results for seedlings grown in well-watered conditions under a PAR of 100 µmol m^{-2} s^{-1}, dry conditions under a PAR of 100 µmol m^{-2} s^{-1}, well-watered conditions under a PAR of 300 µmol m^{-2} s^{-1}, and daughter cladodes in a custom Plexiglass chamber were analysed independently using the same analyses as described above. All 24 h measurements for each individual seedling or cladode were plotted together, with the *y*-axis being the photosynthesis rate [in micromoles of CO_2 per metre squared per second for seedlings and ΔCO_2 (in parts per million) for daughter cladodes] and *x*-axis as time (in hours:minutes:seconds). All 24 h measurements were aligned to the time point at which the attached light sensor recorded a PAR of 0 µmol m^{-2} s^{-1}. Simple linear regression analysis was performed for each of the 24 h measurements and categorized by cladode length, which represents the calculated total diel carbon assimilated for each cladode length measured (net micromoles of CO_2 per metre squared for seedlings and net parts per million of CO_2 for daughter cladodes). Each plot was split into light periods and dark periods (~12 h each) separately. Simple linear regression analysis of the light and dark period plots reflected the total carbon assimilated in the light or the dark, respectively. Lastly, the calculated diel, light and dark total carbon assimilated were plotted vs. measured cladode length for each measurement, in order to visualize trends in carbon fixation as *O. ficus-indica* cladodes grew.

To determine the growth rate of the central cladode in seedlings, the measured cladode length was plotted against its age (in days after germination) using simple linear regression analysis. The slope of the line was used to calculate cladode growth rate under PAR of 100 and 300 µmol m^{-2} s^{-1} (Supplementary data Fig. S2). The rate of seedling cladode length increase was found to decrease transiently as the cotyledons began to senesce. Therefore, the primary cladode length growth rate was calculated by determining the slope of the plotted line before cotyledon senescence began, which was determined by photographs and by the initial decrease and reduction in combined cotyledon length vs. days after germination.

To determine the growth rate of daughter cladodes during the sample period, the length of each daughter cladode was recorded and plotted against its age (in days after germination). All raw data are presented in Supplementary data Table S1.

RESULTS

CAM development in seedlings

Opuntia ficus-indica seedlings were grown in well-watered conditions, under 100 µmol m^{-2} s^{-1} PAR and 20 °C constant temperature. Cotyledons showed increased titratable acidity values at dawn compared with dusk at all stages of development, but these differences were not significant as determined by Welch's *t*-test (Fig. 1A). In primary emergent cladodes, increased dawn titratable acidity values were evident at all stages of development, which became significant at 75 and 100 days after germination as determined by Welch's *t*-test (Fig. 1A). Seedling age, tissue type and time of day all had a highly significant effect on titratable acidity, with the interaction of days after germination with tissue type also having a significant effect on tissue acidity variance (Table 1).

In *O. ficus-indica* seedlings, mean $\delta^{13}C$ values became less negative with seedling development in both cotyledons and primary cladodes (Fig. 1B). For cotyledons, the mean values changed from −21.4 to −17.1 ‰ from 30 to 100 days of age, respectively. For developing primary cladodes, the mean values changed from −19.4 to −14.5 ‰ from 30 to 100 days of age, respectively. These values were significantly different between cotyledons and primary cladodes at 30, 75 and 100 days (but not at 50 days) after germination. The more negative $\delta^{13}C$ ‰ values of the cotyledons were consistent with their lower dawn/dusk titratable acidity values. Linear regression analysis of the change in $\delta^{13}C$ ‰ over the course of seedling growth revealed that the slopes between cotyledons and primary cladodes differed, but that this difference was not significant.

Next, 24 h gas exchange experiments were performed on developing *O. ficus-indica* seedlings grown in well-watered conditions under 100 µmol m^{-2} s^{-1} PAR and 20 °C constant temperature. During early development (<3.7 cm), primary cladode net CO_2 assimilation was negative, but it became positive during phases I and IV of CAM in the night and day, respectively, with increasing cladode length (Fig. 2A). Linear regression analysis of net CO_2 assimilation showed that the transition from negative to positive assimilation occurred when the primary cladodes reached >3.1 cm in length (Fig. 2B). Daytime assimilation rates were significantly lower than nighttime/diel CO_2 assimilation rates ($P < 0.0001$; Fig. 2B).

The experiment was repeated with seedlings grown in water-deficit stress conditions at 100 µmol m^{-2} s^{-1} PAR and 20 °C constant temperature. As the primary cladode grew in length from 0.0 (cotyledons only) to 7.0 cm, CO_2 assimilation patterns were similar to those observed in well-watered seedlings, with net CO_2 assimilation being the greatest during phases I and IV of CAM (Fig. 3A). Linear regression analysis of net CO_2 assimilation showed that the transition from negative to positive assimilation occurred when the primary cladodes reached >3.7 cm in

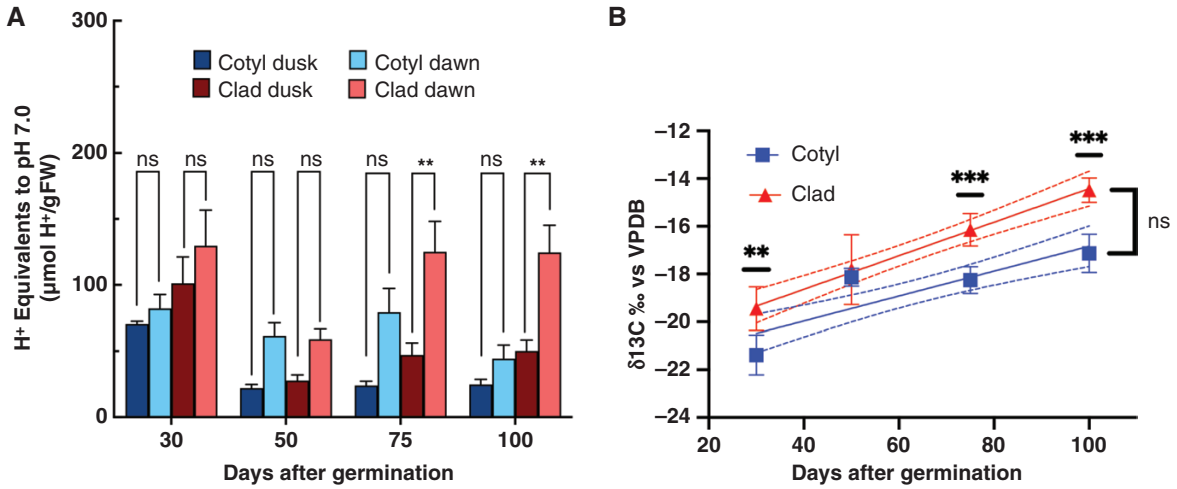

FIG. 1. *Opuntia ficus-indica* seedling titratable acidity (A) and $\delta^{13}C$ values (B) during seedling development in cotyledons (Cotyl) and primary cladodes (Clad) at 100 µmol m^{-2} s^{-1} PAR in well-watered conditions. (A) Titratable acidity [in micromoles of H^+ per gram fresh weight (FW)] of cotyledons and primary cladodes was sampled at dusk and dawn (as indicated in the key) at 30, 50, 75 and 100 days after germination. The significance of comparisons are the results of independent Welch's paired *t*-tests (significance taken as $P < 0.05$; $n = 5$–10). (B) The ^{12}C:^{13}C isotope ratio ($\delta^{13}C$ ‰ vs. VPDB) values of seedling cotyledons and primary cladodes at 30, 50, 75 and 100 days after germination. The significance of comparisons between seedling cotyledons and primary cladodes was determined by independent Welch's paired *t*-tests (significance taken as $P < 0.05$; $n = 5$). Linear regression analysis of the change in $\delta^{13}C$ ‰ over time shows the 95% confidence intervals (dashed lines) and revealed that the slopes between seedling cotyledons ($y = -0.05209x - 22.05$) and primary cladodes ($y = -0.07030x - 21.45$) were not significantly different. Abbreviations: ns, not significant; $^{**}P < 0.01$; and $^{***}P < 0.001$.

TABLE 1. *Three-way ANOVA results of titratable acidity (in micromoles of H^+ per gram fresh weight) of cotyledons and cladodes, sampled at dusk and dawn, at 30, 50, 75 and 100 days after germination*

Source of variation	Percentage of total variation	*P*-value	*P*-value summary	Significant?
Days after germination	10.87	<0.0001	****	Yes
Cotyledon vs. cladode	9.076	<0.0001	****	Yes
Dusk vs. dawn	15.84	<0.0001	****	Yes
Days after germination × cotyledon vs. cladode	3.636	0.0428	*	Yes
Days after germination × dusk vs. dawn	2.46	0.1337	ns	No
Cotyledon vs. cladode × dusk vs. dawn	1.018	0.1275	ns	No
Days after germination × cotyledon vs. cladode × dusk vs. dawn	1.327	0.3848	ns	No

ns, not significant; $^{*}P$ <0.05; $^{****}P$ <0.000.

length, indicating a slight delay compared with well-watered seedlings (Fig. 3B). The overall net assimilation was reduced slightly compared with seedlings grown in well-watered conditions at 100 µmol m^{-2} s^{-1} PAR (Fig. 2). The sample number for these seedlings was limited by technical issues involving CO_2 leaks.

Next, 24 h gas exchange experiments were performed on developing *O. ficus-indica* seedlings grown in well-watered conditions at 300 µmol m^{-2} s^{-1} PAR and 20 °C constant temperature. This higher light intensity resulted in an increased CO_2 assimilation rate during phases I and IV of CAM (Fig. 4A) compared with well-watered seedlings grown under 100 µmol m^{-2} s^{-1} PAR (Fig. 2A). As the primary cladode grew, the net CO_2 assimilation remained negative until the primary cladode reached ~5 cm in length and nighttime net CO_2 assimilation became positive (Fig. 4B). Under higher light conditions, cotyledon senescence was observed; something that was never observed under lower light conditions. However, the occurrence of cotyledon senescence was inconsistent, meaning that no clear-cut statements can be made about this phenomenon. Linear regression analysis revealed that the average cladode growth rate (before cotyledon senescence) was 0.101 (±0.017) and 0.124 (±0.027) cm day^{-1} for seedlings grown under PAR 100 and 300 µmol m^{-2} s^{-1}, respectively (Supplementary data Fig. S2). However, these rates were not significantly different ($P = 0.2078$).

CAM development in daughter cladodes

In addition to seedlings, we also examined titratable acidity and mean $\delta^{13}C$ values in developing daughter cladodes grown in greenhouse conditions. Daughter cladodes <2.5 cm in length showed dawn/dusk titratable acidity differences typical of CAM, with these values becoming significant once the daughter cladodes grew >2.5 cm in length (Fig. 5A). The significance comparisons within each daughter size class were performed

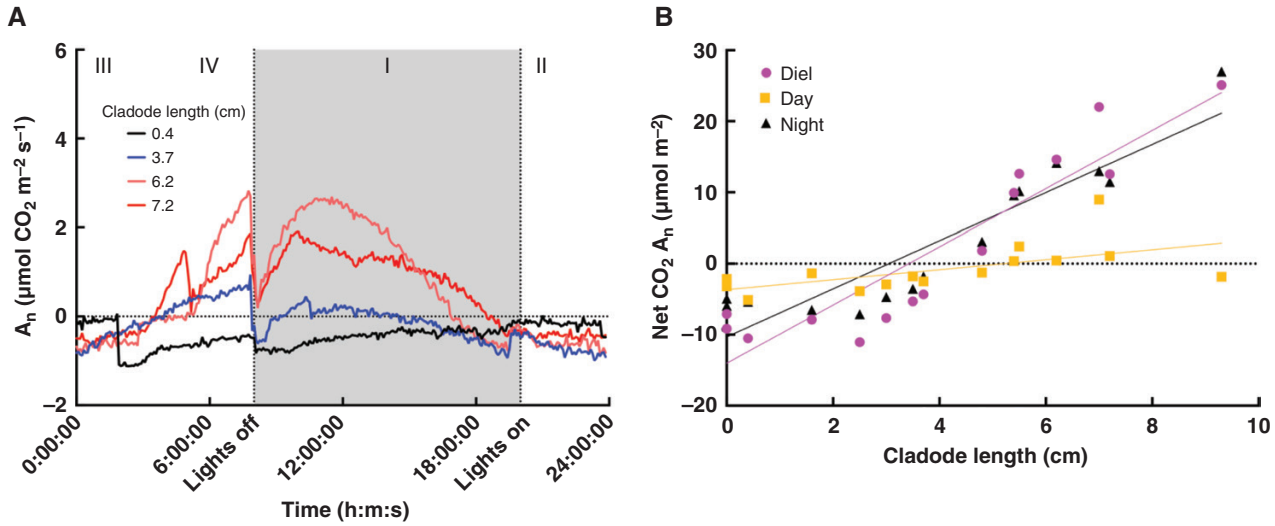

FIG. 2. *Opuntia ficus-indica* seedling diel gas exchange (A) and combined diel gas exchange (B) values during development at 100 μmol m^{-2} s^{-1} PAR in well-watered conditions. (A) Twenty-four hour gas exchange measurements of *O. ficus-indica* seedling 3 as the primary cladode grew, at 0.4, 3.7, 6.2 and 7.2 cm in length. The assimilation rate (in micromoles of CO_2 per metre squared per centimetre) was logged every 5 min. (B) The combined diel, light and dark net assimilated CO_2 (in micromoles per square metre) vs. cladode length (in centimetres) in all well-watered seedlings grown under 100 μmol m^{-2} s^{-1} PAR at 20 °C ($n = 4$). Linear regression analysis revealed that the differences between the slopes for the diel ($y = -4.090x - 14.01$), day ($y = -0.07025x - 3.661$) and night ($y = -3.381x - 10.31$) measurements were extremely significant ($P < 0.0001$). The 95% confidence intervals were not included here, in order to reduce the complexity of the presentation.

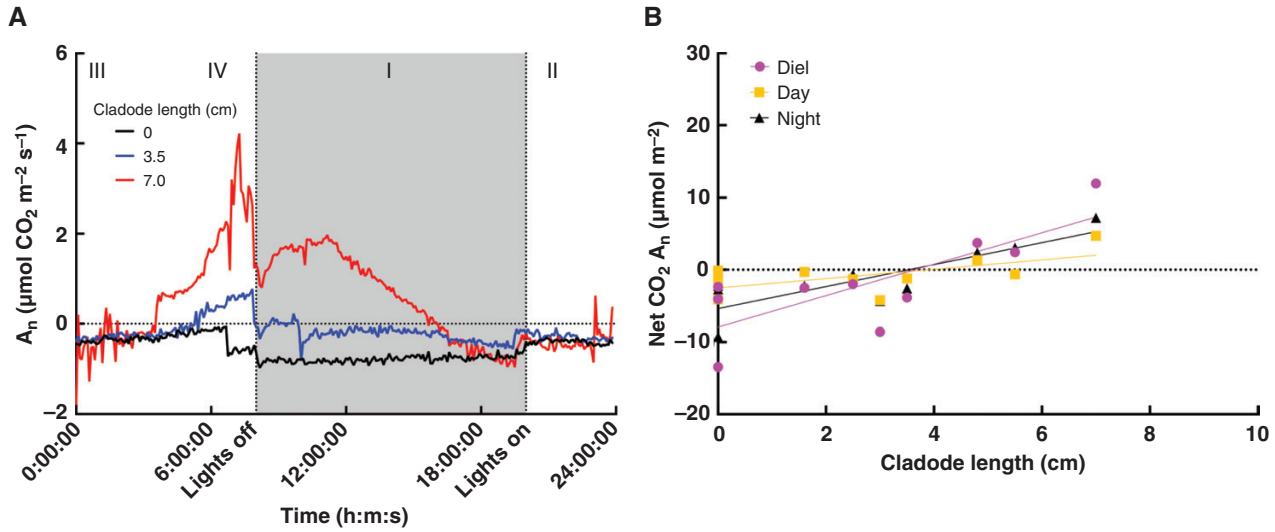

FIG. 3. *Opuntia ficus-indica* seedling diel gas exchange (A) and combined diel gas exchange values (B) during development at 100 μmol m^{-2} s^{-1} PAR in water-deficit stress conditions. (A) Twenty-four hour gas exchange measurements of *O. ficus-indica* seedling 5 as the primary cladode grew, at 0.0, 3.5 and 7.0 cm in length. The assimilation rate (in micromoles of CO_2 per metre squared per centimetre) was logged every 5 min. (B) The combined diel, light and dark net assimilated CO_2 (in micromoles per metre squared) vs. cladode length (in centimetres) in all water-deficit stressed seedlings grown under 100 μmol m^{-2} s^{-1} PAR at 20 °C ($n = 10$). Linear regression analysis revealed that the differences between the slopes for the diel ($y = -2.181x - 7.956$), day ($y = -0.6498x - 2.537$) and night ($y = -1.525x - 5.392$) measurements were not significant ($P = 0.0723$). The 95% confidence intervals were not included here, in order to reduce the complexity of the presentation.

using independent Welch's paired *t*-tests ($P < 0.05$). The mean $\delta^{13}C$ values for daughter cladodes changed from −14.7 ‰ in 12–14 cm cladodes to −15.3 ‰ in 14–16 cm cladodes and −16.1 ‰ in adult cladodes (Fig. 5B). Linear regression analysis of the change in $\delta^{13}C$ ‰ over development showed a trend towards more negative $\delta^{13}C$ values, but an ANOVA with a Brown–Forsythe or Bartlett's test showed that these differences were not significant ($P = 0.08$) owing to heterogeneity of within-group variances and variance across the different developmental stages. However, Tukey's multiple comparison test revealed differences among the different length classes as indicated and that the adult cladodes (~35 cm) showed more negative $\delta^{13}C$ ‰ values than the set of developing daughter cladodes (Fig. 5B).

Next, 24 h gas exchange experiments were performed on developing *O. ficus-indica* daughter cladodes grown in

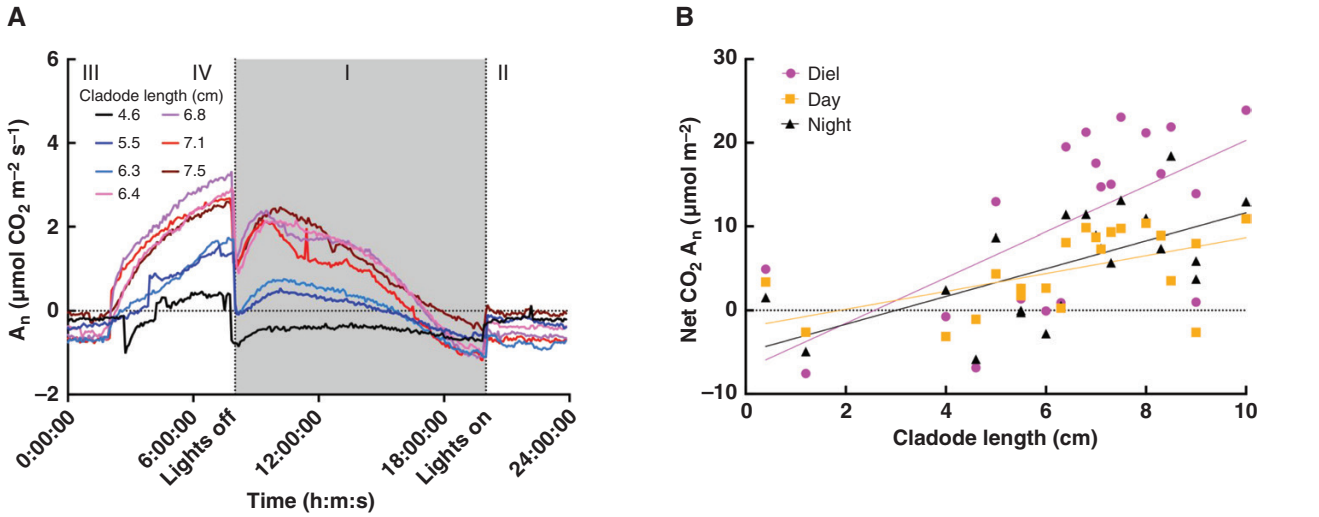

FIG. 4. *Opuntia ficus-indica* seedling diel gas exchange (A) and combined diel gas exchange values (B) during development at 300 μmol m^{-2} s^{-1} PAR in well-watered conditions. (A) Twenty-four hour gas exchange measurements of *O. ficus-indica* seedling 9 as the primary cladode grew, at 4.6, 5.5, 6.3, 6.4, 6.8, 7.1 and 7.5 cm in length. The assimilation rate (in micromoles of CO_2 per metre squared per centimetre) was logged every 5 min. (B) The combined diel, light and dark net assimilated CO_2 (in micromoles per metre squared) vs. cladode length (in centimetres) in all water-deficit stressed seedlings grown under 300 μmol m^{-2} s^{-1} PAR at 20 °C ($n = 4$). Linear regression analysis revealed that the differences between the slopes for the diel ($y = 2.730x - 7.015$), day ($y = -1.069x - 2.011$) and night ($y = 1.661x - 4.983$) measurements were not significantly different ($P = 0.1180$). The 95% confidence intervals were not included here, in order to reduce the complexity of the presentation.

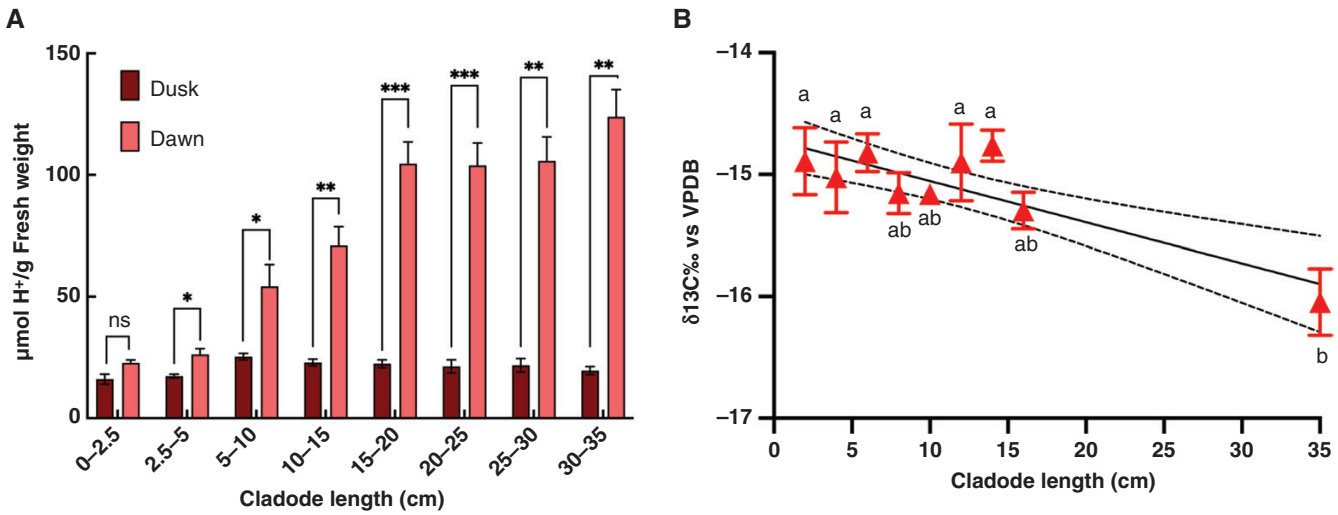

FIG. 5. *Opuntia ficus-indica* daughter cladode titratable acidity (A) and $\delta^{13}C$ values (B) during development. (A) Tissue acidity (in micromoles of H^+ per gram fresh weight) of *O. ficus-indica* daughter cladode tissues collected at dusk and dawn. The significance of comparisons are the results of independent Welch's paired *t*-tests (significance is taken as $P < 0.05$; ns, not significant; $^*P < 0.05$; $^{**}P < 0.01$; and $^{***}P < 0.001$; error bars represent s.e.m.; $n = 2$–6). (B) Measured ^{12}C:^{13}C isotope ratio ($\delta^{13}C$ ‰ vs. VPDB) of daughter cladodes of increasing length classes of 0–2, 2–4, 4–6, 6–8, 8–10, 10–12, 12–14 and 14–16 cm during development, and fully developed (adult ~ 35 cm) cladodes. Linear regression analysis of the changes in $\delta^{13}C$ ‰ over development showed the 95% confidence intervals (dashed lines) and revealed a slope of $y = -0.04272x - 14.66$. ANOVA with a Brown–Forsythe or Bartlett's test showed that these differences were not significant ($P = 0.08$) owing to heterogeneity of within-group variances and variance across the different developmental stages ($n = 6$).

greenhouse conditions. Initially, daughter cladodes showed no recognizable net CO_2 uptake over the 24 h measurement period (Fig. 6A). However, as the daughter cladodes emerged and grew larger, the net CO_2 assimilation rates were observed to increase in both the daytime and nighttime during phases I, II, and IV of CAM once they reached >10 cm in length (Fig. 6A). The net diel, nighttime and daytime CO_2 assimilation rate transitioned to net positive CO_2 assimilation rates when the daughter cladodes reached ~12 cm in length or greater; however, linear regression analysis revealed that the slopes among the three curves were not significantly different (Fig. 6B). Daughter cladodes showed a linear growth trend, with an average growth rate of 1.0 (±0.22) cm day^{-1} (Supplementary data Fig. S3).

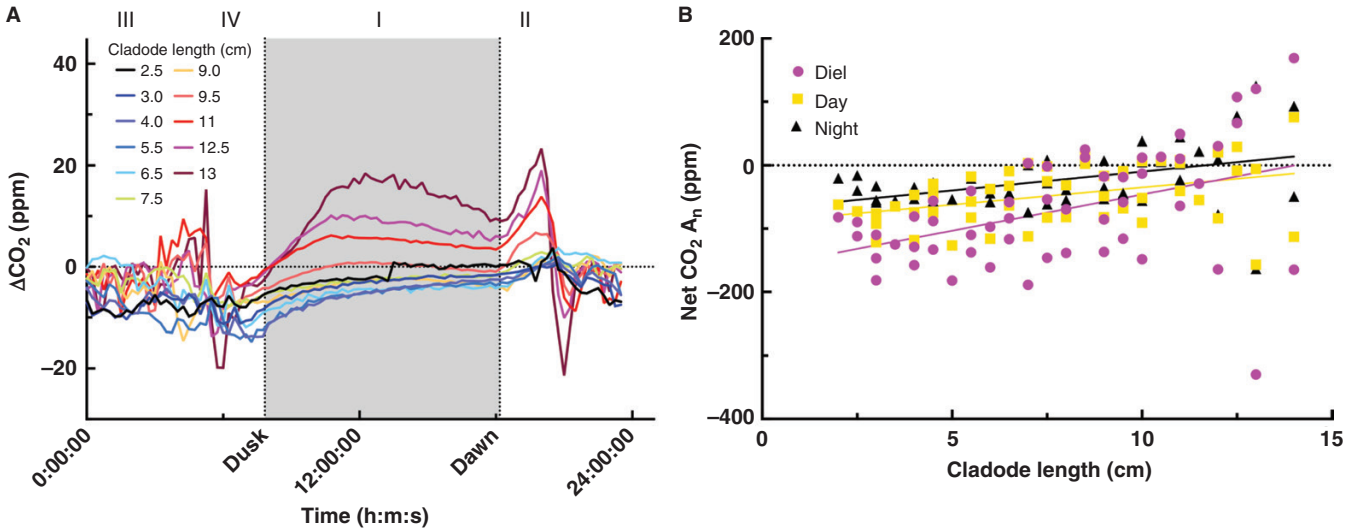

FIG. 6. *Opuntia ficus-indica* daughter cladode 24 h gas exchange measurements (A) and combined diel gas exchange values (B) during development. (A) Twenty-four hour gas exchange measurements of *O. ficus-indica* daughter cladode 4 in the custom-built chamber as the cladode grew, at 2.5, 3.0, 4.0, 5.5, 6.5, 7.5, 9.0, 9.5, 11, 12.5 and 13 cm (colour-coded in the key) in length during development. The ΔCO_2 (in parts per million) was equal to $[CO_2]$ in the reference chamber minus $[CO_2]$ in the sample chamber and was logged every 10 min. (B) Combined diel, light and dark net assimilated CO_2 (in parts per million) vs. cladode length (in centimetres) of *O. ficus-indica* daughter cladodes grown in standard greenhouse conditions ($n = 5$). Linear regression analysis revealed that the differences between the slopes for the diel ($y = 11.44x - 160.5$), day ($y = 5.472x - 89.57$) and night ($y = 5.962x - 69.49$) measurements were not significant ($P = 0.1668$). The 95% confidence intervals were not included here, in order to reduce the complexity of the presentation.

DISCUSSION

The results demonstrate that *O. ficus-indica* seedlings and daughter cladodes engage in CAM from the earliest stages of development. This conclusion is based upon the observation of nocturnal acidification from the earliest stages of cotyledon and cladode seedling development. These results were similar to those obtained in earlier studies based upon dawn/dusk titratable acidity experiments using columnar and barrel cacti species within the Cactaceae, which also occupy arid environments and perform CAM from the earliest stages of development (Altesor *et al.*, 1993; Hernández-González and Villarreal, 2007). The titratable acidity observations were reinforced by $\delta^{13}C$ values obtained from seedlings, whose mean values ranged from −21.4 to −17.1 ‰ for cotyledons and from −19.4 to −14.5 ‰ for cladodes. These ranges of values were well within the range of typical obligate CAM species (O'Leary, 1988) and similar to *O. ficus-indica* mature cladode $\delta^{13}C$ values, which ranged from −13.6 to −11.7 ‰ (Ziegler, 1996; Nogués *et al.*, 2008).

We validated these observations by examining the 24 h gas exchange patterns in *O. ficus-indica* seedlings at 100 and 300 µmol m^{-2} s^{-1} PAR in well-watered conditions and at 100 µmol m^{-2} s^{-1} PAR in water-deficit stress conditions. This relatively low light condition was selected because *Opuntia* seedlings typically grow better in shaded conditions or under the canopy of a nurse plant, which helps their survival (Del Carmen Mandujano *et al.*, 1998; Delgado-Sánchez *et al.*, 2013). Seedling growth research is also conducted under relative low light conditions (i.e. 40 µmol m^{-2} s^{-1}) (Podda *et al.*, 2017). The gas exchange results showed that seedlings did not conduct net positive CO_2 assimilation until the primary cladode reached ~5 cm in length at ~78–90 days after germination, depending upon light conditions (Supplementary data Fig. S2). At this developmental stage, the nighttime CO_2 assimilation typically surpassed that occurring during the daytime, indicative of CAM performance. Before this developmental stage, net CO_2 assimilation was negative. These results with *O. ficus-indica* seedlings are in contrast to those obtained from the tropical epiphytic *O. elatior* seedlings, which showed an initial pattern of C_3 photosynthetic CO_2 assimilation (Winter and Holtum, 2011). Specifically, *O. elatior* seedlings showed CAM phase II net CO_2 assimilation at dawn, whereas this assimilation pattern was never observed in *O. ficus-indica* seedlings. However, *O. ficus-indica* seedlings did exhibit positive CO_2 assimilation rates during phase IV, but only when the cladode reached >3.5–3.7 cm in length (Figs 2–4). These differences are likely to be attributable to *O. ficus-indica* being a terrestrial species adapted to arid regions, with high water-use efficiency requirements, whereas the epiphytic *O. eliator* is adapted to the forest canopy, where more humid conditions are likely to prevail.

Complete drying of the soil for 24 h before conducting gas exchange measurements resulted in a slight reduction in overall CO_2 assimilation rates. However, CO_2 assimilation rates during CAM phases I and IV were largely unchanged from those observed in seedlings not subjected to drying. In contrast, water-deficit stress treatment of *O. elatior* seedlings for several days resulted in increased nighttime CO_2 assimilation, indicative of a facultative CAM component in this species (Winter and Holtum, 2011). A facultative component in *O. ficus-indica* seedlings would probably be more difficult to reveal because *O. ficus-indica* seedlings fixed CO_2 predominantly at night when >4 cm in length in all gas exchange experiments. Indeed, a prolonged water-deficit stress of 4–6 days was required for net nighttime CO_2 assimilation to exceed that of daytime CO_2 assimilation in developing *O. ficus-indica* seedlings, with a marked reduction in daytime CO_2 assimilation (Winter *et al.*, 2008).

In addition to seedlings, we also evaluated the development of CAM in emergent daughter cladodes to search for evidence of C_3 photosynthesis. Initially, we evaluated the presence of CAM using titratable acidity measurements and found that emerging *O. ficus-indica* daughter cladodes displayed nocturnal tissue acidity at all stages, with differences between dawn and dusk being significant when the cladodes were only 2.5–5.0 cm in length. The performance of CAM at the earliest stages of development was reinforced by mean $\delta^{13}C$ values that ranged from −14.0 to −16.0 ‰. These values are indicative of a 'strong' CAM species (O'Leary, 1988) and similar to values from mature cladodes of *O. ficus-indica* $\delta^{13}C$ values, which ranged from −13.6 to −11.7 ‰ when measured *in situ* under ambient CO_2 levels (Ziegler, 1996; Nogués *et al.*, 2008). These results were also corroborated by 24 h gas exchange measurements of the developing cladodes, which showed net negative CO_2 fixation until the daughter cladodes were ~10 cm in length. Before this developmental stage, the emerging cladodes serve as sink tissues that metabolize resources partitioned from the mother cladode, releasing more CO_2 than fixed by either CA/PEPC or RuBisCO. After this stage, the net CO_2 fixation by the cladodes occurred predominantly in CAM phases I and II. The mature adult cladodes showed slightly more negative $\delta^{13}C$ values (ranging from −15.2 to −17.1 ‰) than the developing daughter cladodes. This tendency might be explained by the continued operation of phase II daytime CO_2 fixation as the cladodes matured (Fig. 6A). These results were consistent with earlier observations that *O. ficus-indica* daughter cladodes did not exhibit net positive CO_2 assimilation until 20 days after their initial appearance and imported carbohydrates from mother cladodes at 25 days after emergence (Wang *et al.*, 1998). Furthermore, 24 h gas exchange measurements showed primarily phase I CO_2 assimilation with some CAM phase IV assimilation after the cladodes reached 28 days of age (Wang *et al.*, 1998). In comparison, our results showed increasing CO_2 assimilation in CAM phases I, II and IV in growing daughter cladodes.

Collectively, this study showed that *O. ficus-indica* seedlings use CAM photosynthesis early in development and that C_3 photosynthesis is not the predominant form of photosynthesis even in well-watered conditions. Furthermore, these results confirmed that daughter cladodes emerge from mother cladodes as sink tissues up to ~10 cm in length, and as they grow larger they fix CO_2 predominantly at night along with net daytime CO_2 assimilation, similar to earlier observations (Winter *et al.*, 2008). Therefore, we conclude that the performance of C_3 photosynthesis alone in developing tissues does not appear to be a major contributing factor to the high productivity of *O. ficus-indica*.

SUPPLEMENTARY DATA

Supplementary data are available at *Annals of Botany* online and consist of the following.

Table S1: raw data summaries for all figures. Figure S1: image of the custom-built gas-exchange chamber for measuring 24 h gas exchange with an *Opuntia ficus-indica* daughter cladode as it grows. Figure S2: growth progression of *Opuntia ficus-indica* daughter cladodes grown under different light intensities. Figure S3: growth progression of *Opuntia ficus-indica* daughter cladodes growing from mature mother cladodes under greenhouse conditions.

FUNDING

This research was funded, in part, by Nevada Agricultural Experimental Station (NEV-0377, NEV-0380) and the National Institute of Food and Agriculture (NIFA), U.S. Department of Agriculture, Sustainable Bioenergy and Bioproducts Challenge Area (Award #2018-68005-27924).

ACKNOWLEDGEMENTS

We would like to thank Charli Faris, Eileen Enriquez, Lisa M. Petrusa and Nathan King for their assistance in running 24 h gas exchange measurements on seedlings. Special thanks to Lisa M. Petrusa for making clarifying comments to the manuscript. The authors declare that there are no conflicts of interest in the conduct of this study.

DATA AVAILABILITY

All raw data are presented in Supplementary data Table S1.

LITERATURE CITED

Altesor A, **Ezcurra E**, **Silva C. 1993**. Changes in the photosynthetic metabolism during the early ontogeny of four cactus species. *Acta Oecologica* **3**: 777–785.

Barker DH, **Seaton GGR**, **Robinson SA. 1997**. Internal and external photoprotection in developing leaves of the CAM plant *Cotyledon orbiculata*. *Plant, Cell & Environment* **20**: 617–624.

Borland AM, **Griffiths H**, **Hartwell J**, **Smith JAC. 2009**. Exploiting the potential of plants with crassulacean acid metabolism for bioenergy production on marginal lands. *Journal of Experimental Botany* **60**: 2879–2896. doi:10.1093/jxb/erp118.

Boxall SF, **Dever LV**, **Kneřová J**, **Gould PD**, **Hartwell J. 2017**. Phosphorylation of phosphoenolpyruvate carboxylase is essential for maximal and sustained dark CO_2 fixation and core circadian clock operation in the obligate crassulacean acid metabolism species *Kalanchoë fedtschenkoi*. *The Plant Cell* **29**: 2519–2536. doi:10.1105/tpc.17.00301.

Boxall SF, **Kadu N**, **Dever LV**, ***et al*. 2020**. *Kalanchoë* PPC1 is essential for crassulacean acid metabolism and the regulation of core circadian clock and guard cell signaling genes. *The Plant Cell* **32**: 1136–1160. doi:10.1105/tpc.19.00481.

Christopher JT, **Holtum JAM. 1996**. Patterns of carbohydrate partitioning in the leaves of Crassulacean acid metabolism species during deacidification. *Plant Physiology* **112**: 393–399. doi:10.1104/pp.112.1.393.

Christopher JT, **Holtum JAM. 1998**. Carbohydrate partitioning in the leaves of Bromeliaceae performing C_3 photosynthesis or Crassulacean acid metabolism. *Australian Journal of Plant Physiology* **25**: 371–376.

Del Carmen Mandujano M, **Montanã C**, **Méndez I**, **Golubov J. 1998**. The relative contributions of sexual reproduction and clonal propagation in *Opuntia rastrera* from two habitats in the Chihuahuan Desert. *Journal of Ecology* **86**: 911–921. doi:10.1046/j.1365-2745.1998.00308.x.

Delgado-Sánchez P, **Yáñez-Espinosa L**, **Jiménez-Bremont JF**, **Chapa-Vargas L**, **Flores J. 2013**. Ecophysiological and anatomical mechanisms behind the nurse effect: which are more important? A multivariate approach for cactus seedlings. *PLoS One* **8**: e81513. doi:10.1371/journal.pone.0081513.

Dever LV, **Boxall SF**, **Kneřová J**, **Hartwell J. 2015**. Transgenic perturbation of the decarboxylation phase of Crassulacean acid metabolism alters physiology and metabolism but has only a small effect on growth. *Plant Physiology* **167**: 44–59. doi:10.1104/pp.114.251827.

Gehrig HH, **Wood J**, **Cushman MA**, **Virgo A**, **Cushman JC**, **Winter K. 2005**. Large gene family of phosphoenolpyruvate carboxylase in the crassulacean acid metabolism plant *Kalanchoe pinnata* (Crassulaceae). *Functional Plant Biology* **32**: 467–472.

Hartwell J, **Dever LV**, **Boxall SF. 2016**. Emerging model systems for functional genomics analysis of Crassulacean acid metabolism. *Current Opinion in Plant Biology* **31**: 100–108. doi:10.1016/j.pbi.2016.03.019.

Hernández-González O, **Villarreal OB. 2007**. Crassulacean acid metabolism photosynthesis in columnar cactus seedlings during ontogeny: the effect of light on nocturnal acidity accumulation and chlorophyll fluorescence. *American Journal of Botany* **94**: 1344–1351.

Herrera A. 2008. Crassulacean acid metabolism and fitness under water deficit stress: if not for carbon gain, what is facultative CAM good for? *Annals of Botany* **103**: 645–653. doi:10.1093/aob/mcn145.

Jones M. 1975. The effect of leaf age on leaf resistance and CO_2 exchange of the CAM plant *Bryophyllum fedtschenkoi*. *Planta* **123**: 91–96.

Males J. 2018. Concerted anatomical change associated with crassulacean acid metabolism in the Bromeliaceae. *Functional Plant Biology* **45**: 681–695. doi:10.1071/fp17071.

Martin CE. 1996. Putative causes and consequences of recycling CO_2 via crassulacean acid metabolism. In: **Winter K**, **Smith JAC** eds. *Crassulacean acid metabolism. Ecological studies*, **Vol. 114**. Berlin, Heidelberg: Springer, 192–203. doi:10.1007/978-3-642-79060-7_13.

Messerschmid TFE, **Wehling J**, **Bobon N**, ***et al***. **2021**. Carbon isotope composition of plant photosynthetic tissues reflects a Crassulacean acid metabolism (CAM) continuum in the majority of CAM lineages. *Perspectives in Plant Ecology, Evolution and Systematics* **51**: 125619.

Ming R, **VanBuren R**, **Wai CM**, ***et al***. **2015**. The pineapple genome and the evolution of CAM photosynthesis. *Nature Genetics* **47**: 1435–1442.

Mooney HA, **Bullock SH**, **Ehleringer JR. 1989**. Carbon isotope ratios of plants of a tropical dry forest in Mexico. *Functional Ecology* **3**: 137–142.

Neupane D, **Mayer JA**, **Niechayev NA**, **Bishop CD**, **Cushman JC. 2021**. Five-year field trial of the biomass productivity and water input response of cactus pear (*Opuntia* spp.) as a bioenergy feedstock for arid lands. *GCB Bioenergy* **13**: 719–741. doi:10.1111/gcbb.12805.

Niechayev NA, **Pereira PN**, **Cushman JC. 2019**. Understanding trait diversity associated with crassulacean acid metabolism (CAM). *Current Opinion in Plant Biology* **49**: 74–85. doi:10.1016/j.pbi.2019.06.004.

Nishida K. 1978. Effect of leaf age on light and dark $^{14}CO_2$ fixation in a CAM plant, *Bryophyllum calycinum*. *Plant and Cell Physiology* **19**: 935–941. doi:10.1093/oxfordjournals.pcp.a075683.

Nogués S, **Aranjuelo I**, **Pardo A**, **Azcón-Bieto J. 2008**. Assessing the stable carbon isotopic composition of intercellular CO_2 in a CAM plant using gas chromatography-combustion-isotope ratio mass spectrometry. *Rapid Communications in Mass Spectrometry* **22**: 1017–1022.

O'Leary MH. 1988. Carbon isotopes in photosynthesis. *BioScience* **38**: 328–336. doi:10.2307/1310735.

Osmond CB. 1978. Crassulacean acid metabolism: a curiosity in context. *Annual Review of Plant Physiology* **29**: 379–414. doi:10.1146/annurev.pp.29.060178.002115.

Osmond CB, **Nott DL**, **Firth PM. 1979**. Carbon assimilation patterns and growth of the introduced CAM plant *Opuntia inermis* in eastern Australia. *Oecologia* **40**: 331–350. doi:10.1007/BF00345329.

Osmond B, **Neales T**, **Stange G. 2008**. Curiosity and context revisited: crassulacean acid metabolism in the Anthropocene. *Journal of Experimental Botany* **59**: 1489–1502.

Ping C-Y, **Chen F-C**, **Cheng T-C**, ***et al***. **2018**. Expression profiles of phosphoenolpyruvate carboxylase and phosphoenolpyruvate carboxylase kinase genes in *Phalaenopsis*, implications for regulating the performance of crassulacean acid metabolism. *Frontiers in Plant Science* **9**: 1587. doi:10.3389/fpls.2018.01587.

Podda L, **Santo A**, **Leone C**, **Mayoral O**, **Bacchetta G. 2017**. Seed germination, salt stress tolerance and seedling growth of *Opuntia ficus-indica* (Cactaceae), invasive species in the Mediterranean Basin. *Flora* **229**: 50–57. doi:10.1016/j.flora.2017.02.002.

Skrzypek G, **Paul D**, **Wojtuń B. 2013**. The altitudinal climatic effect on the stable isotope compositions of *Agave* and *Opuntia* in arid environments – a case study at the Big Bend National Park, Texas, USA. *Journal of Arid Environments* **92**: 102–112. doi:10.1016/j.jaridenv.2013.02.002.

Wai CM, **VanBuren R**, **Zhang J**, ***et al***. **2017**. Temporal and spatial transcriptomic and microRNA dynamics of CAM photosynthesis in pineapple. *The Plant Journal* **92**: 19–30.

Walter A, **Christ MM**, **Rascher U**, **Schurr U**, **Osmond B. 2008**. Diel leaf growth cycles in *Clusia* spp. are related to changes between C_3 photosynthesis and crassulacean acid metabolism during development and during water stress. *Plant, Cell & Environment* **31**: 484–491. doi:10.1111/j.1365-3040.2008.01777.x.

Wang N, **Zhang H**, **Nobel PS. 1998**. Carbon flow and carbohydrate metabolism during sink-to-source transition for developing cladodes of *Opuntia ficus-indica*. *Journal of Experimental Botany* **49**: 1835–1843. doi:10.1093/jxb/49.328.1835.

Winter K. 1985. Crassulacean acid metabolism. In: **Barber J**, **Baker NR**, eds. *Photosynthetic mechanisms and the environment*. Amsterdam: Elsevier, 329–387.

Winter K, **Holtum JAM. 2002**. How closely do the $\delta^{13}C$ values of Crassulacean acid metabolism plants reflect the proportion of CO_2 fixed during day and night? *Plant Physiology* **129**: 1843–1851. doi:10.1104/pp.002915.

Winter K, **Holtum JAM. 2011**. Drought-stress-induced up-regulation of CAM in seedlings of a tropical cactus, *Opuntia elatior*, operating predominantly in the C_3 mode. *Journal of Experimental Botany* **62**: 4037–4042.

Winter K, **Smith JAC. 2022**. CAM photosynthesis: the acid test. *New Phytologist* **233**: 599–609.

Winter K, **Foster JG**, **Schmitt MR**, **Edwards GE. 1982**. Activity and quantity of ribulose bisphosphate carboxylase- and phosphoenolpyruvate carboxylase-protein in two Crassulacean acid metabolism plants in relation to leaf age, nitrogen nutrition, and point in time during a day/night cycle. *Planta* **154**: 309–317. doi:10.1007/BF00393908.

Winter K, **Garcia M**, **Holtum JAM. 2008**. On the nature of facultative and constitutive CAM: environmental and developmental control of CAM expression during early growth of *Clusia*, *Kalanchoë,* and *Opuntia*. *Journal of Experimental Botany* **59**: 1829–1840. doi:10.1093/jxb/ern080.

Winter K, **Holtum JAM**, **Smith JAC. 2015**. Crassulacean acid metabolism: a continuous or discrete trait? *New Phytologist* **208**: 73–78. doi:10.1111/nph.13446.

Yang X, **Hu R**, **Yin H**, ***et al***. **2017**. The *Kalanchoë* genome provides insights into convergent evolution and building blocks of crassulacean acid metabolism. *Nature Communications* **8**: 1899.

Ziegler H. 1996. Carbon- and hydrogen-isotope discrimination in crassulacean acid metabolism. In: **Winter K**, **Smith JAC**, eds. *Crassulacean acid metabolism. Ecological studies*, **Vol. 114**. Berlin, Heidelberg: Springer, 336–348.